Role of nitrogen in the formation of hard and elastic CN_x thin films by reactive magnetron sputtering

Niklas Hellgren,* Mats P. Johansson, Esteban Broitman, Lars Hultman, and Jan-Eric Sundgren
Department of Physics, Linköping University, S-58183 Linköping, Sweden
(Received 16 June 1998)

Carbon nitride films, deposited by reactive dc magnetron sputtering in Ar/N_2 discharges, were studied with respect to composition, structure, and mechanical properties. CN_x films, with $0 \leqslant x \leqslant 0.35$, were grown onto Si (001) substrates at temperatures between 100 and 550 °C. The total pressure was kept constant at 3.0 mTorr with the N_2 fraction varied from 0 to 1. As-deposited films were studied by Rutherford-backscattering spectroscopy, x-ray photoelectron spectroscopy, electron-energy loss spectroscopy, Raman and Fourier transform infrared spectroscopy, and nanoindentation. Three characteristic film structures could be identified: For temperatures below ~150 °C, an amorphous phase forms, the properties of which are essentially unaffected by the nitrogen concentration. For temperatures above ~200 °C, a transition from a graphitelike phase to a ''fullerenelike'' phase is observed when the nitrogen concentration increases from ~5 to ~15 at. %. This fullerenelike phase exhibits high hardness values and extreme elasticity, as measured by nanoindentation. A ''defected-graphite'' model, where nitrogen atoms goes into substitutional graphite sites, is suggested for explaining this structural transformation. When a sufficient number of nitrogen atoms is incorporated, formation of pentagons is promoted, leading to curving of the basal planes. This facilitates cross-linking between the planes and a distortion of the graphitic structure, and a strong three-dimensional covalently bonded network is formed. [S0163-1829(99)03808-4]

I. INTRODUCTION

Carbon nitride compounds with ~20 at. % nitrogen have been found to exhibit very interesting properties, such as high hardness combined with an extreme elasticity. Such material can be synthesized, e.g., by dc magnetron sputtering from a graphite target in both pure N_2 and mixed Ar/N_2 discharges, provided that the growth temperature is at least 200 °C.[1,2] The combination of a hard and at the same time an elastic material has been attributed to a ''fullerenelike'' microstructure, with curved and intersecting basal planes, giving rise to a strong, yet flexible, three-dimensional covalently bonded network.[1] It was suggested that the incorporation of nitrogen promotes formation of pentagons in the otherwise hexagonal graphitelike planes, and thus induces buckling of the basal planes which facilitates cross-linking between the planes through sp^3-coordinated carbon. Similar microstructure, with curved and intersecting basal planes, and with similar mechanical behavior, has also been observed in pure carbon films, provided that the available energy is high enough to form pentagons in the structure.[3] However, in the case of sputtered films, nitrogen is believed to play an important role in the formation of this structure. Also, for the amorphous phase, the incorporation of nitrogen has been shown to improve some properties of the film, particularly their tribological properties.[4,5]

In this study, we have prepared CN_x films with x ranging from 0 to 0.35, at substrate temperatures between 100 and 550 °C, in order to study the role of nitrogen in the formation of hard and elastic covalently bonded networks. The films were analyzed with respect to their composition, chemical structure, and mechanical properties, and the results are correlated to the microstructure of the films. The results obtained are in support of the structural model proposed by Sjöström *et al.*,[1] and a more detailed phenomenological description for how the films form is presented.

II. EXPERIMENTAL DETAILS

CN_x films were deposited by unbalanced reactive dc magnetron sputtering in mixed Ar/N_2 discharges. The target was a high-purity 99.99% pyrolytic graphite disc, 75 mm in diameter, mounted on the cathode at a distance of ~10 cm from the rotatable substrate table. The base pressure of the deposition chamber was $\sim 1 \times 10^{-9}$ Torr (1.3×10^{-7} Pa). Pure argon and nitrogen (both 99.9999% purity) were introduced into the process chamber through mass flow controllers, and the total pressure was monitored by a capacitance manometer. A series of deposition was done with the total pressure kept constant at 3.0 mTorr (0.4 Pa) and with the N_2 fraction varied from 0 to 1. In the case of very low N_2 partial pressure ($\leqslant$0.5%), the nitrogen was introduced through a high-precision needle valve and the gas mixture was monitored by a differentially pumped quadrupole mass spectrometer. Depositions were made with substrate temperatures T_s of 100, 350, and 550 °C, as monitored by a calibrated thermocouple in the substrate holder. The effect of plasma heating (radiation from the plasma, bombardment of energetic particles, etc.) of the substrate was accounted for in the reported values.

The substrates were Si (001) wafers, which were cleaned ultrasonically in acetone and alcohol, in sequence, prior to being load-locked into the deposition chamber. Polished graphite discs, with a surface roughness R_a of ~1 nm, were also used as substrates for the Rutherford-backscattering spectroscopy (RBS) measurements. After the substrates were introduced into the deposition chamber, residual surface oxides were removed by heating the substrates to 850 °C for 10 min. Before the deposition was initiated, the target was sputter cleaned for ~10 min with a shutter covering the substrate. Depositions were made with a constant magnetron current of 0.3 A, which required a discharge voltage of ~560 V, independent on the gas mixture. The substrates were kept

at negative floating potential V_f, which was found to be ~25–30 V. With a plasma potential V_p of ~10–15 eV, as measured by a Langmuir probe, this corresponds to an incident N_2^+ ion energy of ~15 eV. All films were grown to a thickness of at least 0.5 μm.

The elemental composition of the as-deposited films was determined by RBS, using a 2-MeV He^+ beam, incident normal to the film surface. The backscattered particles were detected at a 150° scattering angle. Graphite substrates were used for this analysis in order to separate the film peaks from the substrate signal. The chemical structure was further analyzed using a VG Microlab 310F combined Auger electron spectroscopy and x-ray photoelectron spectroscopy (XPS) system. Immediately after taken out of the deposition chamber, the samples were loaded into the analysis chamber. As-received samples were analyzed by XPS and reflection electron energy-loss spectroscopy (REELS), without any initial sputter etching. XPS was carried out using a nonmonochromated Mg K_α (1253.6 eV) x-ray source and a hemispherical electron energy analyzer. The energy analyzer energy was set such that the Au $(4f_{7/2})$ line was recorded with a full width at half maximum (FWHM) of ~0.9 eV. REELS was measured in the low-loss region, using a 1.5-keV incident electron beam energy, and a spectral resolution of ~0.8 eV. A take-off angle of 90° was used for both the XPS and REELS measurements.

Raman spectroscopy was carried out on a Dilor XY800 instrument, using the 514.5-nm Ar laser line, and a spectral resolution of ~3 cm^{-1}. Fourier transform infrared (FTIR) spectroscopy was done in transmittance mode using a Bruker IFS66 spectrometer.

In order to evaluate the mechanical response of the film, nanoindentation experiments were carried out using a Nano Indenter™ II instrument. Indentations were made by a trigonal (Berkovich) diamond tip using a single loading-unloading cycle. A 100-s constant-load hold segment was used at 70% unload to allow any thermal drift of the instrument to be measured and corrected for. Indentations were made with maximum loads of 1, 3, 5, and 10 mN, with at least 5 indents sequences for each load. The Indenter tip shape had been calibrated following the procedure described in Ref. 6, and the calibration was frequently checked by measuring on a fused silica sample.

The stress level in the films was evaluated using the substrate curvature method, which has been described elsewhere.[7] Films were deposited on 0.38-mm-thick Si (001) substrates (12×12 mm squares), and the curvature, as well as the film thickness, was determined using a stylus profilometer.

III. RESULTS

The nitrogen concentration in the films as a function of nitrogen partial pressure and temperature is displayed in Fig. 1. For all temperatures, the amount of nitrogen incorporated in the film C_N increased rapidly with only a few percent of N_2 in the sputtering gas. However, when more N_2 was added to the gas mixture, C_N saturated rather quickly at a temperature-dependent level. The maximum amount of nitrogen in the films was found to be 26, 20, and 17 at. % for T_s=100, 350, and 550 °C, respectively. The situation of a

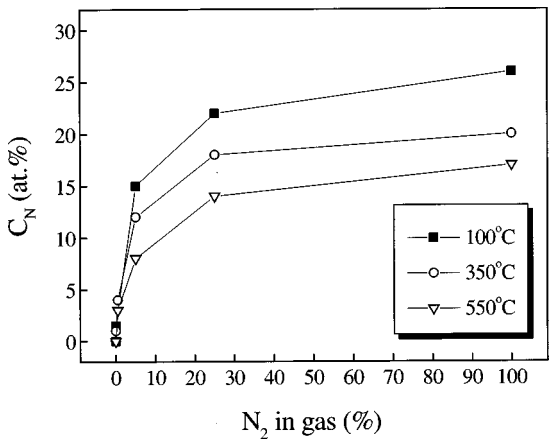

FIG. 1. The nitrogen concentration C_N in the film as a function of the percentage of N_2 in the sputtering gas, for growth temperatures of 100, 350, and 550 °C.

maximum nitrogen concentration that decreases with increased temperature has been reported by several authors,[8–10] and can be explained by an increased desorption of volatile nitrogen-rich CN species, such as C_2N_2, at higher temperatures.[11,12]

The chemical structure was analyzed by XPS. Overview spectra showed that only small amounts of oxygen (<2 at. % in the surface layers) was adsorbed on the sample surface during transport from the deposition chamber to the analysis chamber. Figures 2(a) and 2(b) show N 1*s* core-level spectra for samples grown at 100 and 350 °C, respectively, and with different nitrogen contents. The spectra have been normalized to the same maximum intensity and a Shirley-type background[13] has been subtracted. For the T_s=100 °C samples [Fig. 2(a)], three spectral contributions can be resolved by the fitting of Gaussian line shapes: one at 400.1 eV (denoted by P_2, FWHM=2.0 eV), one at 398.2 eV (P_3, FWHM=1.9 eV), and a small contribution at ~402 (P_1, FWHM=2.2 eV). For the films deposited at 350 °C [Fig. 2(b)] and 550 °C (not shown), the two main peaks, P_2 and P_3, are shifted apart from each other and are found at 400.6 (FWHM=1.9 eV) and 398.1 eV (FWHM=1.9 eV), respectively. This shift in binding energy with increasing temperature can be related to a change in microstructure, as previously observed by high-resolution TEM.[14] In addition, the best fit for the 350 and 550 °C samples is obtained if a fourth peak P_4 is added at 399.0 eV (FWHM=1.0 eV). All this is in agreement with previously reported results.[15] It can clearly be seen that when increasing the nitrogen concentration in the films grown at elevated temperatures, P_3 grows with respect to P_2. In the case of the samples grown at T_s =100 °C, the same effect can be observed, however, not as pronounced. The same trend has also been reported by Souto *et al.* for rf sputtered CN_x films with x ranging from 0.1 to 0.43.[16]

The assignments of the N 1*s* peaks diverge somewhat between different authors. However, it is now generally agreed that the peak P_2 can be assigned to nitrogen bonded to sp^2-coordinated carbon, e.g., as substitutional N in a graphite sheet. P_3, on the other hand, is assigned to nitrogen bond to sp^3-hybridized carbon.[15,17] This interpretation is also supported by *ab initio* binding-energy calculations.[16,18] The

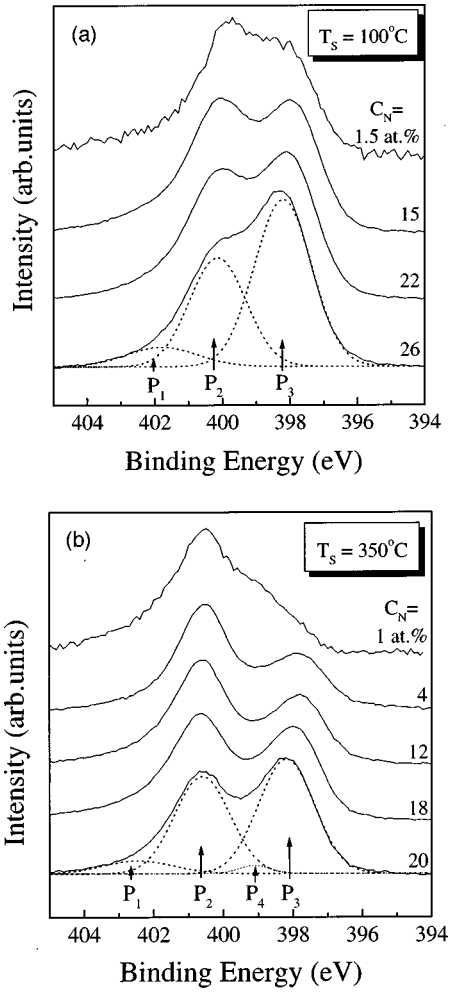

FIG. 2. XPS N 1*s* spectra of CN_x films with various nitrogen content, grown at (a) $T_s = 100\,^{\circ}\mathrm{C}$ and (b) $T_s = 350\,^{\circ}\mathrm{C}$. The spectra have been normalized to the same maximum intensity and a Shirley-type background has been subtracted.

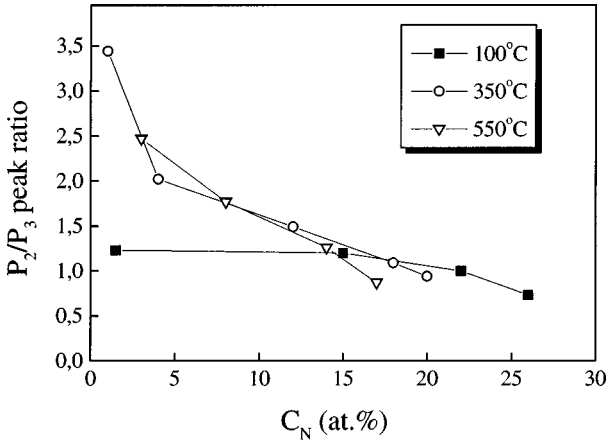

FIG. 3. Ratios between the P_2 and P_3 N 1*s* peak components, corresponding to nitrogen bond to sp^2- and sp^3-coordinated carbon, respectively, as a function of the nitrogen concentration in CN_x thin films.

peak P_4 has been suggested to correspond to nitrogen triple bonded to carbon. However, recent calculations[18] show that P_4 might also arise from pyridinelike nitrogen, i.e., N bonded to two sp^2-coordinated C atoms at the edge of a graphite sheet. The peak P_1 is generally attributed to N-O bonds in the surface layer. However, since that peak also can be seen after that all oxygen is removed by sputter etching, it is likely that nitrogen bond to carbon in some other chemical environment also contributes in that energy region. The calculations referred to above indicate that the N 1*s* binding energy is very sensitive to the exact chemical environment of the N atom.[18]

Figure 3 shows the P_2/P_3 peak ratio as a function of nitrogen concentration in the film. It can be seen that for $T_s = 100\,^{\circ}\mathrm{C}$, the ratio stays fairly constant at ~ 1, with only a slight decrease with increasing C_N. In the case of higher T_s, the P_2/P_3 ratio decreased monotonically from about 3 to 1 with increasing C_N. This means, if the peak assignment is correct, that the first nitrogen atoms go into sites where they bond only to sp^2-coordinated carbon atoms, but when more nitrogen is incorporated into the compound, some of the N will bond to sp^3 carbon. This does not necessarily mean that the number of tetrahedral carbon increases with increasing C_N, but just that more nitrogen goes into sites next to sp^3-coordinated carbon atoms. The spectrum from the film with $C_N = 1$ at. %, grown at $T_s = 350\,^{\circ}\mathrm{C}$ [Fig. 2(b)], also indicates that the peak P_4 grows with respect to P_3 when the nitrogen concentration decreases. This implies that if P_4 corresponds to pyridinelike nitrogen, the ratio between N bonded to sp^2- and sp^3-coordinated carbon, respectively, is even higher than what is indicated in Fig. 3, for low nitrogen concentrations.

Since the C 1*s* XPS peaks appeared broad and rather featureless, only with an asymmetry on the higher binding-energy side indicating carbon in at least three different binding states, it is difficult to draw any conclusions about the sp^2/sp^3 fractions from the C 1*s* peak. Instead, reflection EELS measurements were applied to study the density of σ- and π-type electrons. A high π-electron signal, observed at ~ 7 eV energy loss, would indicate a high density of unsaturated carbon bonds, i.e., sp^2- and sp^1-hybridized carbon, while the absence of a π resonance would mean a purely sp^3-coordinated structure. Figure 4 shows REELS spectra from selected CN_x films, and, for comparison, spectra from pure graphite and diamond. It can be observed that the π signal, for the samples grown at elevated temperatures, indeed decreases with increased C_N. For the pure carbon films, the π-electron densities appear to be comparable to that of graphite, while for the films with maximum C_N, the π signal is somewhere between that of graphite and diamond. In the case of the low-T_s samples, the π signal does not change significantly with the nitrogen concentration. The trends for the REELS spectra are consistent with those observed for the XPS N 1*s* peaks at different temperatures. Thus, it seems that the change in the P_2/P_3 ratio with C_N is really associated with a change in the amount of sp^3-hybridized carbon in structure. Furthermore, both Raman and FTIR measurements showed only a weak signal at $\sim 2210\ \mathrm{cm}^{-1}$, corresponding to the C≡N stretching mode (i.e., carbon in the sp^1 state). This further indicates that the nitrogen atoms are predominantly bonded to sp^2- and sp^3-coordinated carbon.

Furthermore, the densities of the films were estimated measuring the position of the $\sigma+\pi$ plasmon peak in the REELS experiments. Assuming a free-electron model, the

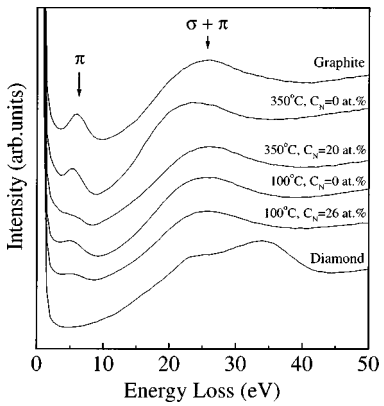

FIG. 4. Reflection EELS low-loss spectra from films grown at $T_s = 100$ and 350 °C in either pure Ar or N_2. Spectra from diamond and graphite are shown for comparison.

plasmon energy is proportional to $n_e^{1/2}$, where n_e is the valence electron density, which can be related to the mass density of the sample.[19] This method cannot be expected to give very accurate values in the case of carbon nitrides, but it gives at least an indication of the trends. It was found that for the $T_s = 100$ °C films, the density was ~2.5 g/cm^3 independently of C_N. For the higher temperatures, the densities were found to increase from ~1.8 g/cm^3 for $C_N = 0$, up to the level of the low-T_s samples for $C_N \geq 10$ at. %. These values can be compared to graphite and diamond, which have densities of 2.25 and 3.5 g/cm^3, respectively.

Previous studies have shown that for films grown in pure nitrogen discharge, two different microstructures can be observed by high-resolution transmission electron microscopy (HREM), depending on T_s.[14] For temperatures below ~150 °C, the microstructure is predominantly amorphous, while for $T_s > 200$ °C, a fullerenelike microstructure is observed, with a high degree of curved and intersecting basal planes. HREM analysis of the present samples further showed that for higher T_s, the structure becomes increasingly ordered. In the case of pure carbon films grown at elevated temperatures, the microstructure appeared somewhat different, with much smaller features of curved basal planes, as will be discussed in more detail in a future publication.

Raman spectroscopy is a commonly used technique to analyze the quality of both artificially grown diamond and various amorphous carbon compounds. Figure 5 shows Raman spectra from the pure carbon films and CN_x films, grown at $T_s = 100$, 350, and 550 °C. The carbon spectra [Fig. 5(a)] are composed of two broad bands centered around 1570 cm^{-1} (G band) and 1360 cm^{-1} (D band). For the nitrogen-containing films [Fig. 5(b)], also a small peak at ~2210 cm^{-1} appears, corresponding to the C≡N stretching mode, as discussed above. It can be seen in Fig. 5 that both the widths and intensities of the G and D peaks change depending on T_s and C_N.

The G band (G for graphite) corresponds to the symmetric E_{2g} vibrational mode in graphitelike materials, while the *D* band (*D* for disorder) arises from the limitations in the graphite domain size, induced by grain boundaries or imperfections, such as substitutional N atoms, sp^3 carbon, or other impurities.[20] Thus, the intensity of the *D* band is quite sensitive to the size of the microdomains, and as the grain size increases the intensity of the *D* band decreases with respect to the G band. The relative Raman intensities of the *D* and G band are therefore a measure of the degree of order in an amorphous carbon sample. The *D*/G peak ratio was extracted from our samples by the fitting of Lorentzian peak shapes. It was found that the ratio, for a fixed temperature, stayed fairly constant when introducing nitrogen in the structure, but when increasing the temperature the ordering in the structure increased. The *D*/G ratio was found to decrease from ~3.5 at $T_s = 100$ °C to ~2.5 at $T_s = 350$ °C, and finally to ~2.0 at $T_s = 550$ °C. Furthermore, the widths of the peaks also give important information about the crystallinity of the films. Amorphous materials give rise to broad, diffuse peaks, while crystalline materials give well-defined sharp peaks. Figure 6 shows the FWHM of the *D* peak as a function of C_N. For the pure carbon films, the width of the *D* peak is considerably lower for higher T_s (which is also evident from Fig. 5), while the difference decreases when nitrogen is incorporated in the films. For $T_s = 100$ °C, the broad *D* peak is indicative of an amorphous microstructure and the incorporation of nitrogen does not seem to change the Raman line shapes essentially. For higher T_s, a gradual peak broadening can be observed when C_N increases, which indicates that the incorporation of N breaks the long-range order of the graphitic structure. The width of the G peak follows the same trend, however, not as pronounced as in the case of the *D* peak. It should be noted

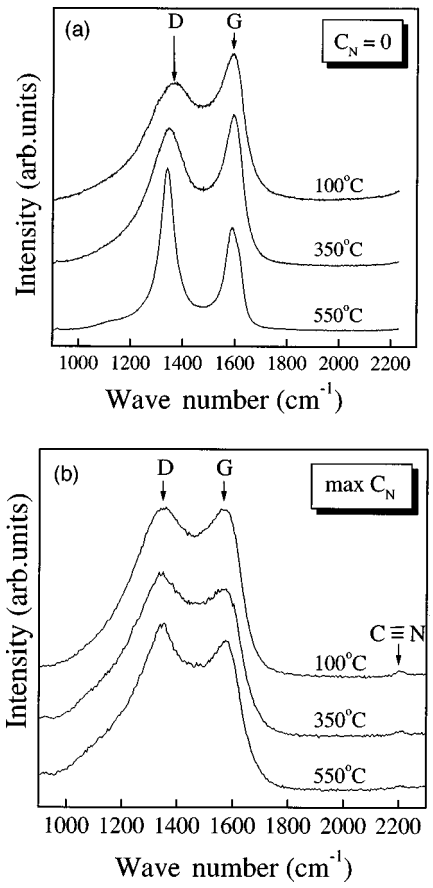

FIG. 5. Raman spectra from (a) the pure carbon films grown at different temperatures, and (b) from the CN_x films grown in pure N_2. The spectra have been normalized to the same maximum intensity.

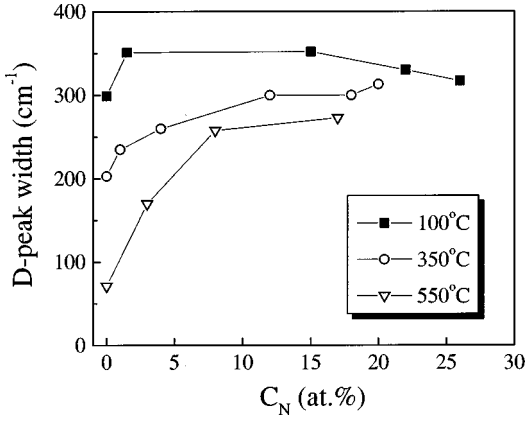

FIG. 6. Full width at half maximum (FWHM) of the Raman *D* peaks, as a function of nitrogen concentration in CN_x films.

that in the case of the nitrogen-containing films, slightly asymmetric line shapes were needed to properly fit the *D* and G peaks. This may be interpreted as additional smaller peaks were present, assumably from C—N bonds, which is consistent with the conclusion that the nitrogen breaks the long-range graphitic order.

Nanoindentation is an attractive technique for analyzing the mechanical properties of thin films independently of the substrate. Figure 7 compares the nanoindentation response from CN_x films grown in pure N_2 at $T_s = 100\,°C$ and $350\,°C$ for a maximum load of 3 mN. The most important difference between those films is the elastic recovery R, defined as $R = (d_{max} - d_{res})/d_{max}$, where d_{max} and d_{res} are the displacement at maximum load and residual displacement after removal of the load, respectively. For the film grown at $350\,°C$, R is as high at 90%, compared to ~75% for the amorphous phase, a value that is comparable to what is commonly seen for amorphous carbon films. The highly elastic response for the $350\,°C$ sample makes calculations of the hardness and Young's modulus difficult. The commonly used method for calculating these quantities assumes that the upper part of the unloading curve can be fitted by a power law,[6] an assumption that does not hold in this case. However, by using a different approach, based on the analysis of the loading curves, the hardness of this highly elastic phase has been estimated to be as high as ~40–60 GPa.[1,14] The hardness of the amorphous phase is, however, possible to estimate, and using the method of Oliver and Pharr,[6] a value of ~20 GPa is obtained. This can be compared to, e.g., commercial polycrystalline TiN coatings, which typically exhibit a hardness of ~25–30 GPa, and elastic recoveries of ~40–50% when measured under similar conditions.[21]

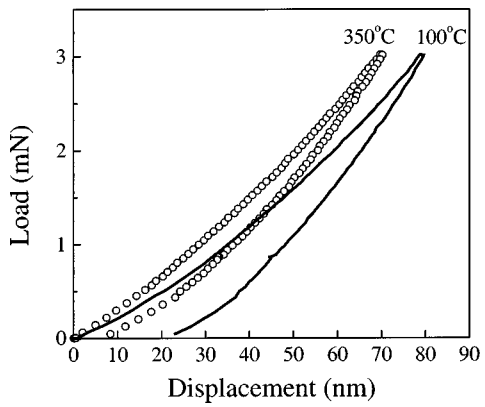

FIG. 7. Nanoindentation load-displacement curves from CN_x films grown in 100% N_2 and at $T_s = 100$ and $350\,°C$, respectively.

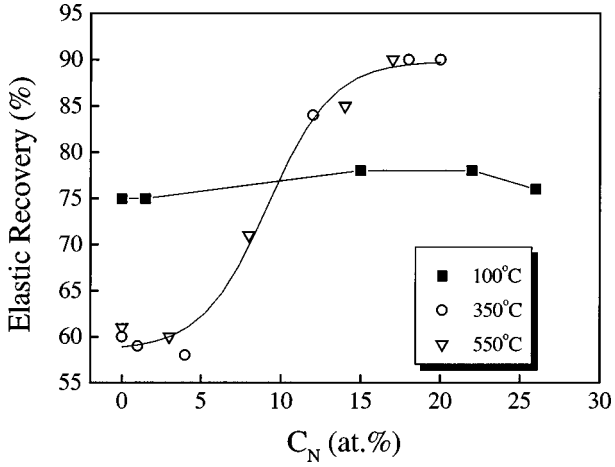

FIG. 8. Elastic recovery, measured by nanoindentation, as a function of the nitrogen concentration in CN_x thin films grown at 100, 350, and $550\,°C$.

The elastic recovery is a characteristic property of the CN_x thin films. Figure 8 shows the variation of this quantity as a function of the amount of nitrogen in the films. It can be seen that for the films grown at higher temperatures, there is a distinct transition to a highly elastic phase when C_N increases above ~5–10 at. %. Correspondingly, the maximum penetration at a fixed load increases dramatically when C_N is reduced below ~12 at. %. In the case of the low-T_s samples, neither the elastic recovery, nor the maximum penetration changes significantly with C_N.

It should be noted that values for the elastic recovery and the maximum penetration can not be directly compared between measurements made by different tips. Those quantities are, especially for small indents, very dependent on the exact tip shape; a sharper tip would give both higher maximum penetration and a smaller elastic recovery, and vice versa for a more blunt tip. However, in this study all samples were measured with the same tip, and the exact tip shape did not change during the measurements, as verified by measuring on a fused silica reference sample.

The film properties were further analyzed by measuring the stress level σ of the as-deposited films. The stresses were found to be compressive in all films, and the results are shown in Fig. 9. Even though the error bars are rather large, the trends can be clearly seen. The stresses in the films grown at $T_s = 350\,°C$ are very low as long as the nitrogen content stays below ~ 5 at. %, but increases rapidly up to ~2.5 GPa when more nitrogen is incorporated. The films grown at $T_s = 550\,°C$ show a similar behavior, however, the maximum stress level is lower. Again, it can be seen that the properties of the low temperature amorphous phase do not change significantly with varying nitrogen concentrations, but the stress stays fairly constant between 1.0 and 1.5 GPa. In agreement with the present results, films grown in pure N_2 discharge have previously been reported to reach a maximum stress level for $T_s \sim 350\,°C$.[22]

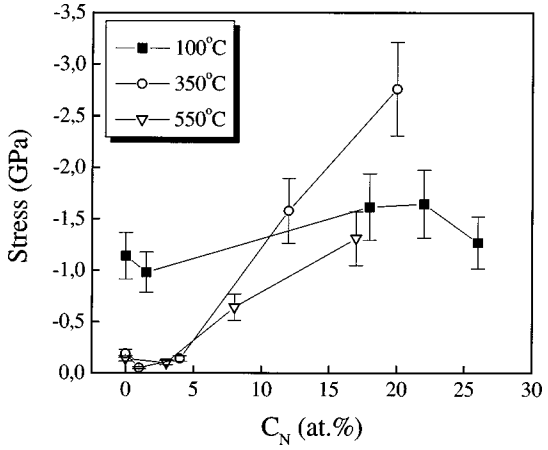

FIG. 9. Stresses in as-deposited CN_x films, as a function of nitrogen concentration.

IV. DISCUSSION

From the present results, three different structures of CN compounds can be identified depending on the growth temperature and nitrogen concentration, as illustrated in Fig. 10: (i) an amorphous phase which forms at low temperatures, (ii) a graphitelike phase which forms at higher temperatures and with low nitrogen concentrations, and (iii) a fullerenelike structure for high temperatures and C_N larger than $\sim$15 at. %. Transition regions are observed between these characteristic structures.

CN_x films grown at temperatures below $\sim 150\,^{\circ}$C, have previously been observed to exhibit an amorphous microstructure.[14] The same is observed for the present samples, and neither of the properties analyzed show any significant change dependent on the amount of nitrogen that is incorporated in the film. XPS and REELS analysis show that there is a significant fraction of sp^3-coordinated carbon in the film, however, the exact sp^3 fraction cannot be accurately calculated from the techniques used. The mechanical properties are comparable to those of amorphous diamondlike carbon.

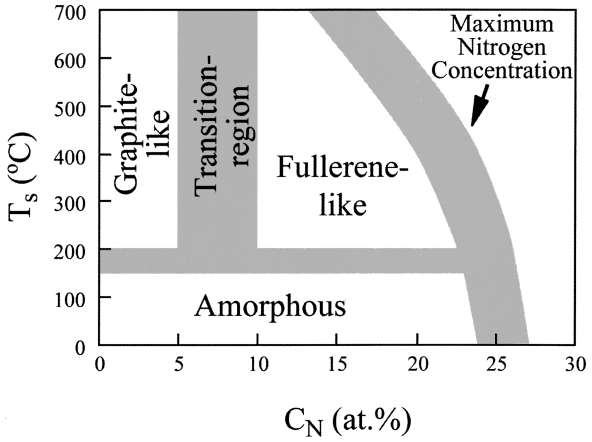

FIG. 10. A diagram over the structures observed in sputtered CN_x films for different substrate temperatures T_s and nitrogen concentrations C_N.

In the case of films grown at elevated temperatures, there is a substantial change in both structure and mechanical properties, depending on the nitrogen concentration in the films. The pure carbon films exhibited a graphitelike microstructure with predominantly sp^2, and possibly also sp^1-coordinated carbon. Raman spectroscopy revealed that the crystalline quality of the graphite improves with higher substrate temperature. The mechanical properties of these films are very poor, as expected for a graphitic material. As nitrogen is being incorporated, XPS analysis show that the first nitrogen atoms preferentially go into sites next to sp^2-hybridized carbon, most likely at substitutional graphite sites. When more nitrogen is incorporated in the films, the number of tetrahedral carbon increases, as determined by XPS and REELS. This phenomena was also recently observed by Souto *et al.*[16] Raman spectroscopy showed an increased disorder in the structure. Furthermore, a substantial improvement in mechanical properties is observed when the nitrogen concentration reaches $\sim$15 at. %. This is also accompanied by a considerable increase of the stresses in the films.

The large change in properties occurring at $C_N \sim 15$ at. % can be explained using the following arguments: A hexagonal graphitic structure represents the structure obtained for the pure carbon films grown at $T_s \geqslant 200\,^{\circ}$C. When a small amount of nitrogen is incorporated in the structure, the N atoms take substitutional positions in the graphite layers, however, without changing the shape or properties of the basal planes essentially, as illustrated in Fig. 11(a). Presumably, the nitrogen atoms are distributed so that initially there is not more than one nitrogen atom per aromatic ring. In that way, if the nitrogen atoms are perfectly distributed, maximum 16.7 at. % ($\frac{1}{6}$) of nitrogen could be incorporated in the structure without changing the graphitic properties. For films with high nitrogen concentration, however, the microstructure with curved basal planes, observed previously by HREM, indicates that odd-membered rings, most likely pentagons, must be incorporated in the structure to facilitate curving. Similar microstructures have been observed also for pure carbon films grown by arc evaporation,[3] a technique similar to what is used for production of fullerene molecules and nanotubes. However, in sputtering techniques, the energy available is normally lower than that required to form pentagons in the structure of pure carbon films. For hydrogen-terminated graphitic sheets with seven hexagons (24 C atoms). Sjöström *et al.* used total-energy calculations to deduce that an energy of 73.8 kcal/mol is required for forming a pentagon in the sheet structure.[1] However, the energy cost decreased by 26.2 kcal/mol if two carbon atoms in the pentagon were substituted by nitrogen atoms.[1] When more than 16.7 at. % of nitrogen is incorporated, there must necessarily be more than one N atom in some graphitic rings, unless nitrogen precipitates to a N-rich phase. This high local concentration of nitrogen would, thus, promote the formation of pentagons, even if the available energy would not be sufficient to form pentagons in a pure graphite structure. The formation of pentagons results in bending of the basal planes, just like in the case of fullerenes, as illustrated in Fig. 11(b). The distance between the basal planes would thereby locally get smaller which would facilitate cross-linking through sp^3-coordinated carbon. This is consistent with the

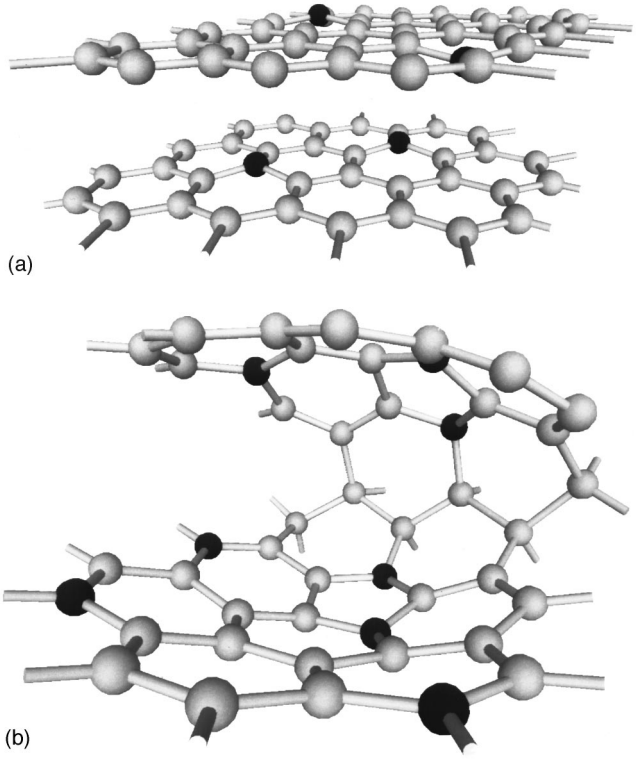

FIG. 11. The transition from a graphitic to a ''fullerenelike'' structure with increasing nitrogen concentration in the films. (a) 5% of nitrogen (darker atoms) is incorporated in a graphite sheet, without changing the graphitic structure. With $C_N \approx 15$ at. %, the nitrogen promotes formation of pentagons which results in buckling of the basal planes (b) and facilitates cross-linking between the planes through sp^3-coordinated carbon.

XPS and EELS results, which show an increased number of sp^3 carbon, and also with the Raman results which indicates an increased disorder in the structure. Also, the fact that the density increases further indicates that the distance between the basal planes decreases. When there is a sufficient degree of strong covalent bonds between the basal planes, the mechanical properties improves considerably, as can be seen from the nanoindentation data. Furthermore, the possibility for a high degree of bond-angle deformation in this kind of structure makes the films highly elastic.

The structural transition to fullerenelike films would, if the nitrogen atoms were perfectly distributed over the graphite sheet, be expected to occur at $C_N \sim 16.7$ at. %. The present results, however, show that there is a transition region between ~5 and 15 at. % of nitrogen. This is, of course, understandable, and can be expected since deviations from a perfectly homogeneous distribution of nitrogen will result in a gradual transition from a graphite structure to a ''fullerenelike'' structure. Also, the possibility that pentagons form when only one N atom is present, must be considered, as well as the fact that the local nitrogen concentration increases when one C atom is removed from the hexagon in the formation of pentagons. At about 17 at. % of nitrogen the transition is completed, which is consistent with the proposed scheme.

The assumption that the nitrogen preferentially is distributed so that there is not more than one N per aromatic ring, is further supported by the fact that the amount of nitrogen that is incorporated in the film saturates at about 15–20 at. % (cf. Fig. 1). C_N increases rapidly when small doses of N_2 are mixed in the sputtering gas, but when the N_2 dose is increased there is already so much nitrogen in the structure that the probability of forming N—N bonds will be high. As N—N bonds form on the growth surface they will most likely immediately be desorbed. Thus, C_N saturates at a level, which corresponds to only slightly more than one nitrogen atom per aromatic ring. It should, however, be noted that the maximum nitrogen concentration obtainable, depends on the exact sputtering geometry, particle energies, and fluxes, etc. As a matter of fact, up to ~30 at. % of nitrogen have been reported for this hard and elastic phase.[8] Also in the case of the amorphous phase a saturation can be expected, however, since the structure is different, the maximum obtainable C_N can be considerably higher.

The scheme proposed here bears similarity with the ''defected graphite model'' for diamondlike carbon, presented by Tamor and Wu.[23] That model used simple arguments to predict densities and optical properties, as a function of the number of defects in both hydrogenated and hydrogen-free amorphous carbon. The ''defects'' in that case were either hydrogen or sp^3-hybridized carbon, while it in our case nitrogen introduces defects and cross-linking through formation of odd-membered rings.

V. CONCLUSIONS

Three characteristic film structures exist for carbon nitride films deposited by reactive dc magnetron sputtering in Ar/N_2 discharges at a constant total pressure and with the N_2 fraction varied from 0 to 1. For temperatures below ~150 °C, an amorphous phase forms. For temperatures above ~200 °C, a transition from a graphitelike phase to a fullerenelike structure is observed when the nitrogen concentration increases from ~5 to ~15 at. %. A ''defected-graphite'' model, where nitrogen goes into substitutional graphite sites and promotes formation of odd-membered rings which, in turn, favors cross-linking through sp^3-coordinated carbon, is suggested for explaining this transition. While the nanoindentation response of the amorphous CN phase is essentially unaffected by the N content, the mechanical properties of the films grown at elevated temperatures improves considerably as the nitrogen content increases above ~10 at. %.

ACKNOWLEDGMENTS

The financial support from the Material Research Consortium on Thin Film Growth through the Swedish Foundation for Strategic Research (SSF) is greatly appreciated. Dr. Sveinn Olafsson at Linköping University, and Joakim Bäckström with co-workers at the Chalmers University of Technology, Sweden, are acknowledged for assistance with RBS and Raman measurements, respectively. Furthermore, Åsa Johansson and Sven Stafström at Linköping University are acknowledged for fruitful discussions concerning the interpretation of the XPS data.

*Corresponding author. Electronic address: nikhe@ifm.liu.se

[1] H. Sjöström, S. Stafström, M. Boman, and J.-E. Sundgren, Phys. Rev. Lett. **75**, 1336 (1995).
[2] H. Q. Lou, N. Axén, R. E. Somekh, and I. M. Hutchings, Diamond Relat. Mater. **5**, 1303 (1996).
[3] G. A. J. Amaratunga, M. Chhowalla, C. J. Kiely, I. Alexandrou, R. Aharonov, and R. M. Devenish, Nature (London) **383**, 321 (1996).
[4] E. C. Cutiongco, L. Dong, W. C. Yip, and C. S. Bhatia, Trans. ASME, J. Tribol. **118**, 543 (1996).
[5] A. Khurshudov, K. Kato, and S. Daisuke, J. Vac. Sci. Technol. A **14**, 2935 (1996).
[6] W. C. Oliver and G. M. Pharr, J. Mater. Res. **7**, 1564 (1992).
[7] C. A. Davis, D. R. McKenzie, Y. Yin, E. Krautchinskaia, G. A. Amaratunga, and V. S. Veerasamy, Philos. Mag. B **69**, 1133 (1994).
[8] W. T. Zheng, H. Sjöström, I. Ivanov, K. Z. Xing, E. Broitman, W. R. Salaneck, J.-E. Greene, and J. E. Sundgren, J. Vac. Sci. Technol. A **14**, 2696 (1996).
[9] D. G. McCulloch and A. R. Merchant, Thin Solid Films **290**, 99 (1996).
[10] M. Chhowalla, I. Alexandrou, C. Kiely, G. A. J. Amaratunga, R. Aharonov, and R. F. Fontana, Thin Solid Films **290**, 103 (1996).
[11] P. Hammer and W. Gissel, Diamond Relat. Mater. **5**, 1152 (1996).
[12] W. T. Zheng, N. Hellgren, H. Sjöström, and J.-E. Sundgren, Surf. Coat. Technol. **100-101**, 287 (1998).
[13] D. A. Shirley, Phys. Rev. B **5**, 4709 (1972).
[14] H. Sjöström, L. Hultman, J.-E. Sundgren, S. V. Hainsworth, T. F. Page, and G. S. A. M. Theunissen, J. Vac. Sci. Technol. A **14**, 56 (1996).
[15] W. T. Zheng, K. Z. Xing, N. Hellgren, M. Lögdlund, Å Johansson, U. Gelius, W. R. Salaneck, and J.-E. Sundgren, J. Electron Spectrosc. Relat. Phenom. **87**, 45 (1997).
[16] S. Souto, M. Pickholz, M. C. dos Santos, and F. Alvarez, Phys. Rev. B **57**, 2536 (1998).
[17] M. A. Baker and P. Hammer, Surf. Interface Anal. **25**, 629 (1997).
[18] Å Johansson and S. Stafström (unpublished).
[19] N. Laidani, A. Miotello, A. Glisenti, C. Bottani, and J. Perriere, J. Phys.: Condens. Matter **9**, 1743 (1997).
[20] J. H. Kaufman, S. Metin, and D. D. Saperstein, Phys. Rev. B **39**, 13 053 (1989).
[21] L. Karlsson, Licentiate thesis No. 633, Linköping University, Sweden, 1998.
[22] E. Broitman, W. T. Zheng, H. Sjöström, I. Ivanov, J. E. Greene, and J.-E. Sundgren, Appl. Phys. Lett. **72**, 2532 (1998).
[23] M. A. Tamor and C. H. Wu, J. Appl. Phys. **67**, 1007 (1990).